Synthesis and crystal structures of copper(II) dinuclear complex and zinc(II) coordination polymer as materials for efficient oxidative desulfurization of dibenzothiophene

Adedibu C. Tella[a,*], Adetola C. Oladipo[a], Vincent O. Adimula[a] , Olanrewaju A. Ameen[a], Susan A. Bourne[b] and Adeniyi S. Ogunlaja[c,*]

[a]Department of Chemistry, P.M.B.1515, University of Ilorin, Ilorin, Kwara State, Nigeria,
[b]Centre for Supramolecular Chemistry Research, Department of Chemistry, University of Cape Town, Rondebosch 7701, South Africa,
[c]Department of Chemistry, Nelson Mandela University, PO Box 77000, Port Elizabeth, 6031, South Africa,
e-mail: ac_tella@yahoo.co.uk and adeniyi.ogunlaja@mandela.ac.za

Supplementary Data

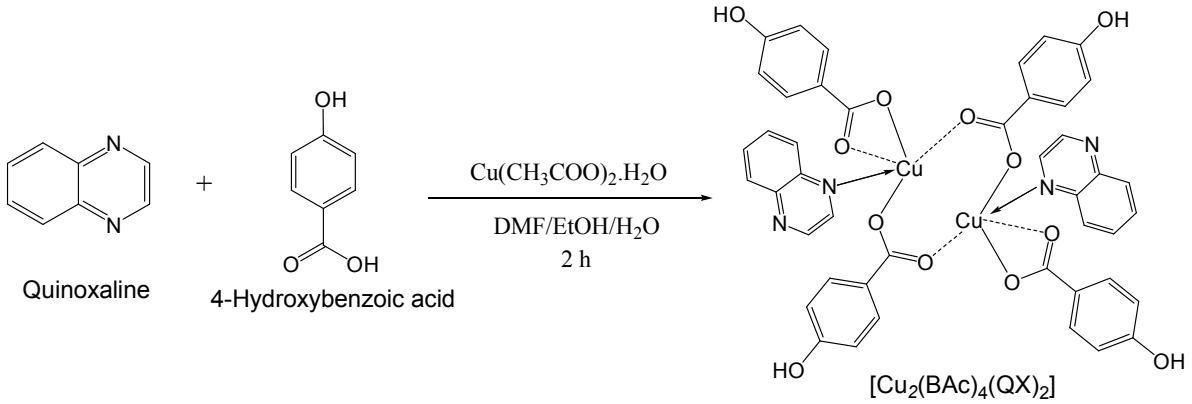

Scheme S1 Reaction scheme for the synthesis of $[Cu_2(BAc)_4(QX)_2]$

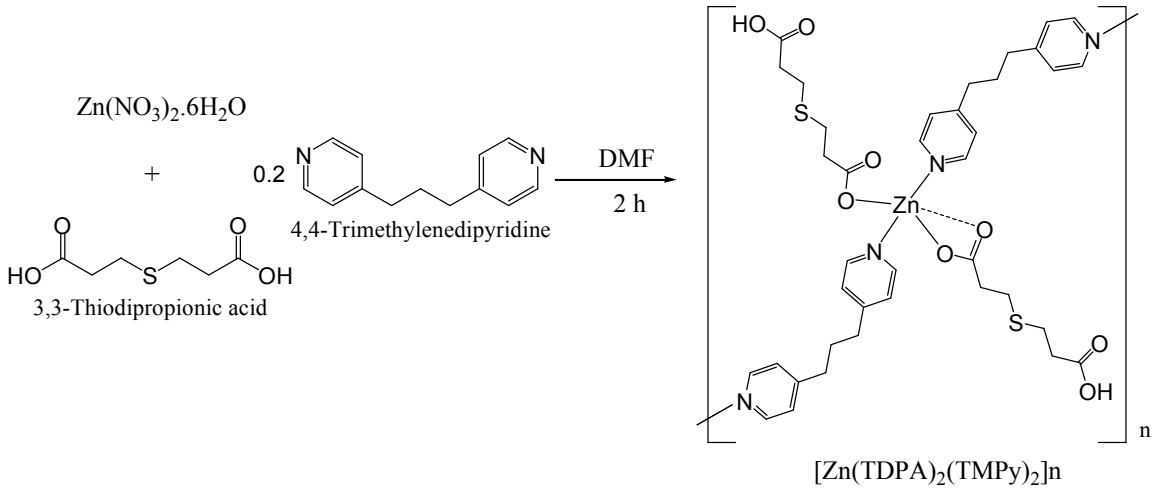

Scheme S2 Reaction scheme for $[Zn(TDPA)_2(TMPy)_2]_n$

1.0 Adsorption experiments

In a typical adsorption experiment, various masses of adsorbent, $[Zn(TDPA)_2(TMPy)_2]_n$, were brought into contact in with DBTO solution (930 mg/L and 3 mL acetonitrile/ n-hexane (1:1)) in a glass vial and stirred at room temperature to attain the adsorption equilibrium. Adsorption progress was monitored by measuring the amount of unadsorbed DBTO *via* the use of GC-FID. Adsorption capacity, q_e (mg g^{-1}), was obtained using Eqn 1.

$$q_e = \frac{V(C_o - C_e)}{W} \qquad (1)$$

(C_o) is the initial concentration (mg L^{-1}), (C_e) is equilibrium concentration (mg L^{-1}), (W) is the weight of $[Zn(TDPA)_2(TMPy)_2]_n$ (g) and (V) volume of solvent in litres). Adsorption kinetics, isotherm and selectivity of DBTO, were also calculated. For selectivity coefficient, Eqn 2 was employed:

$$\alpha_{a\text{-}b} = (q_a / q_b) \div (C_{e,a} / C_{e,b}) \qquad (2)$$

where q_a and q_b are adsorption capacities (mg g^{-1}) of compound a and reference compound b at equilibrium, respectively. $C_{e,a}$ and $C_{e,b}$ (mg L^{-1}) are equilibrium concentrations of compound a and reference compound b, respectively [1]. Naphthalene (NAP) was selected as a reference compound as it is a predominant poly aromatic hydrocarbon (PAH) present in fuel.

2.0 Computational Methods

To accelerate the adsorption calculation, a unit of the Coordination polymer, $[Zn(TDPA)_2(TMPy)_2]_n$, was extracted for binding energy (BE) calculations at LanL2DZ /BY3LP level using the Gaussian program (calculated at 298K) [2-4]. The BEs could be defined as shown below (Eqn 3):

Adsorbent + Adsorbate → Adsorbate:Adsorbent

$$BE = E_{(adsorbent:adsorbate)} - E_{(adsorbent)} - E_{(adsorbate)} \qquad (3)$$

where $E_{(adsorbent:adsorbate)}$ is the energy of the $[Zn(TDPA)_2(TMPy)_2]_n$-DBTO sorption system at the equilibrium state, while $E_{(adsorbent)}$ and $E_{(adsorbate)}$ are the total energy of $[Zn(TDPA)_2(TMPy)_2]_n$ and the DBTO, respectively.

Further ab-initio calculations such as HOMO energy (E_{HOMO}), LUMO energy (E_{LUMO}), LUMO-HOMO energy gap (ΔE), hardness (η), softness (σ), electronegativity (χ) and chemical potential (μ), $I = -E_{HOMO}$, $A = -E_{LUMO}$ were calculated using equations 4-7:

$$\eta = \frac{I - A}{2} \quad (4)$$

$$\sigma = \frac{1}{\eta} \quad (5)$$

$$\chi = \frac{I + A}{2} \quad (6)$$

$$\mu = -\chi \quad (7)$$

First-order molecular hyperpolarizability (β_0), dipole moment (μ) and polarizability (α_0) are modelled using the the equation below,

$$\mu = (\mu^2_x + \mu^2_y + \mu^2_x)^{1/2}$$

$$\alpha_0 = (\alpha_{xx} + \alpha_{yy} + \alpha_{zz})/3$$

$$\beta_0 = (\beta^2_x + \beta^2_y + \beta^2_z)^{1/2}$$

where,

$$\beta_x = \beta_{xxx} + \beta_{xyy} + \beta_{xzz}$$

$$\beta_y = \beta_{yyy} + \beta_{xxy} + \beta_{yzz}$$

$$\beta_z = \beta_{zzz} + \beta_{xxz} + \beta_{yyz}$$

Table S1 Relevant crystal data and data collection summary

	$[Cu_2(BAc)_4(QX)_2]$ (1)	$[Zn(TDPA)_2(TMPy)_2]_n$ (2)
Formula	C_{44} H_{32} Cu_2 N_4 O_{12}	$(C_{19}H_{22}N_2O_4$ SZn)n·0.2(H_2O)
Formula weight	935.81	443.12
Crystal system	Monoclinic	Monoclinic
Space group	P 21/c (14)	C 2/c
a (Å)	9.7035 (7)	18.8659 (13)
b(Å)	18.8466(14)	13.3682 (9)
c(Å)	10.6948(8)	17.1126(12)
α (°)	90	90
β (°)	102.326(2)	107.432(3)
γ (°)	90	90
V ($Å^3$)	1910.8 (2)	4117.6 (5)
Z	2	8
Temperature (K)	173	300
Crystal color	Blue	Colourless
Crystal Shape	Prism	Plate
Crystal Size [mm]	0.18 x 0.22 x 0.54	0.19 x 0.32 x 0.41
F000	956.0	1838.0
Radiation (Å)	MoKa 0.71073	MoKa 0.71073
h,k,l_{max}	12, 25, 14	25, 17, 22
N_{ref}	4777	5153
T_{min},T_{max}	0.759, 0.887	0.760, 0.853
Max. and min. transmission	0.887 and 0.759	0.853 and 0.760
Θ_{max} (°)	28.387	28.364
Data completeness	0.999	0.998
N_{par}	288	264
R(reflections)	0.0282(3966)	0.0702 (3616)
wR_2(reflections)	0.0645(4777)	0.2455 (5153)

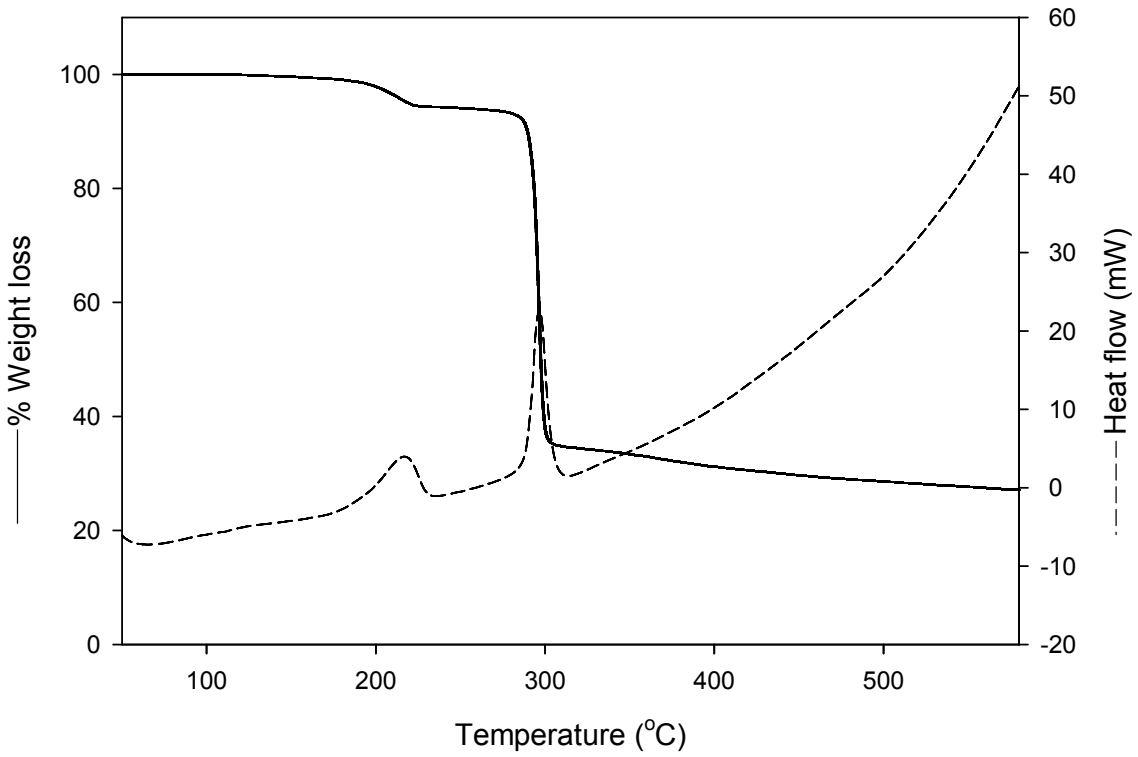

Fig. S1. TGA-DSC profiles of $[Cu_2(BAc)_4(QX)_2]$

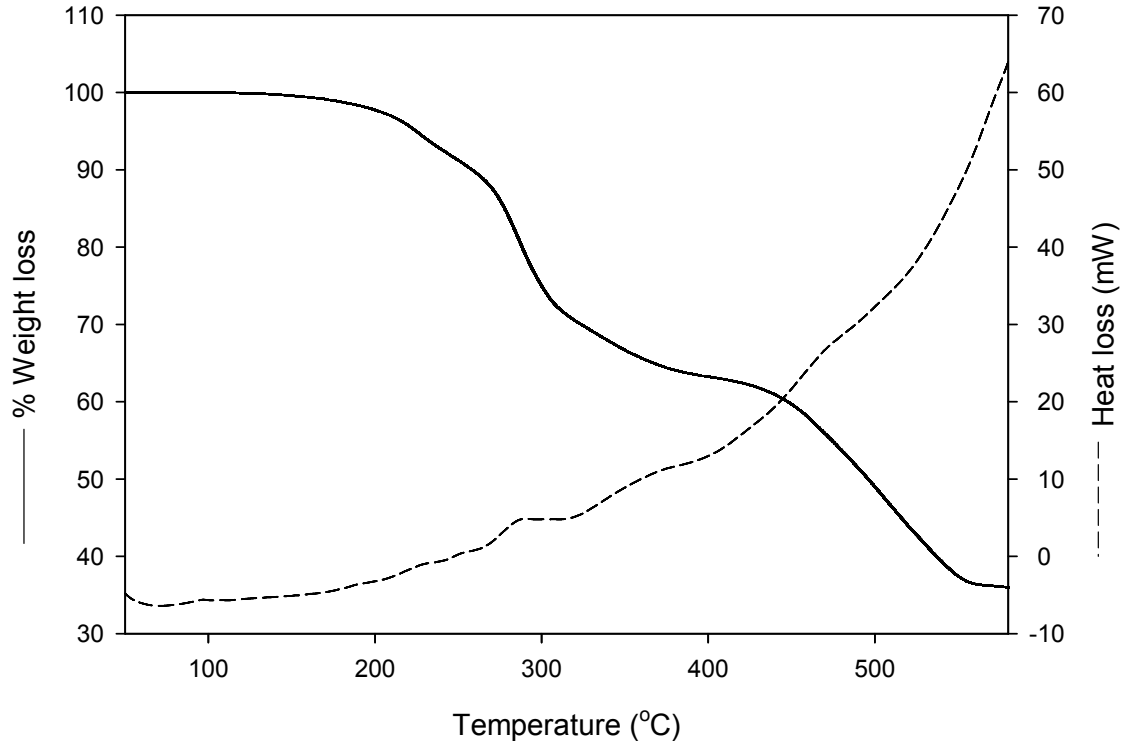

Fig. S2. TGA-DSC profiles of $[Zn(TDPA)_2(TMPy)_2]_n$

A

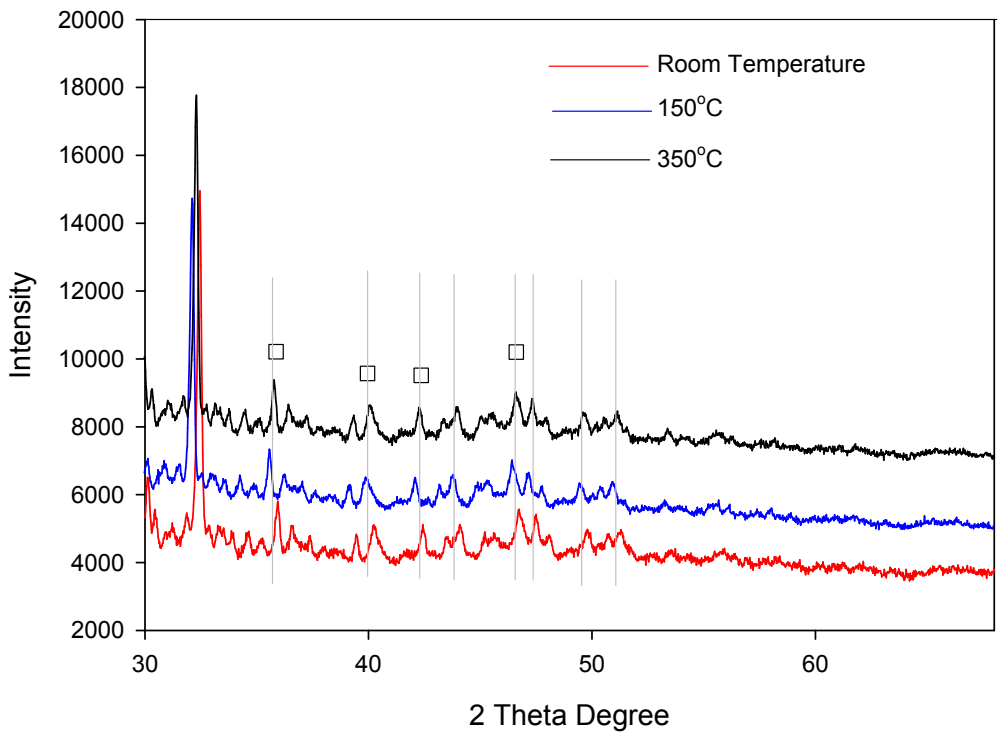
Room Temperature
150°C
350°C
Intensity
2 Theta Degree
20000
18000
16000
14000
12000
10000
8000
6000
4000
2000
30
40
50
60

B

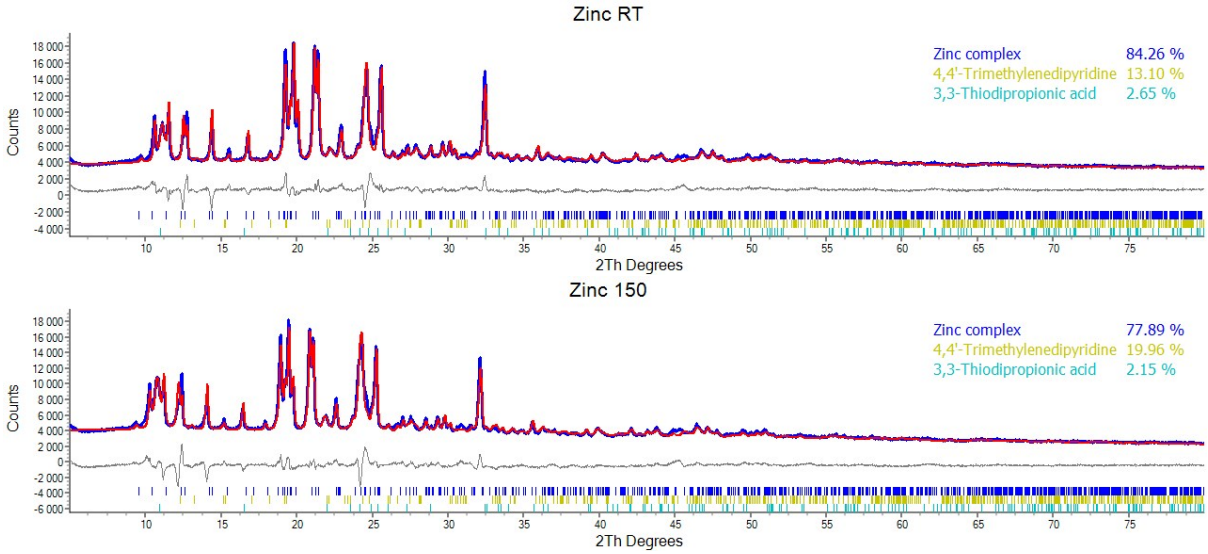
Zinc RT
Zinc complex 84.26 %
4,4'-Trimethylenedipyridine 13.10 %
3,3-Thiodipropionic acid 2.65 %
Counts
2Th Degrees
Zinc 150
Zinc complex 77.89 %
4,4'-Trimethylenedipyridine 19.96 %
3,3-Thiodipropionic acid 2.15 %
Counts
2Th Degrees

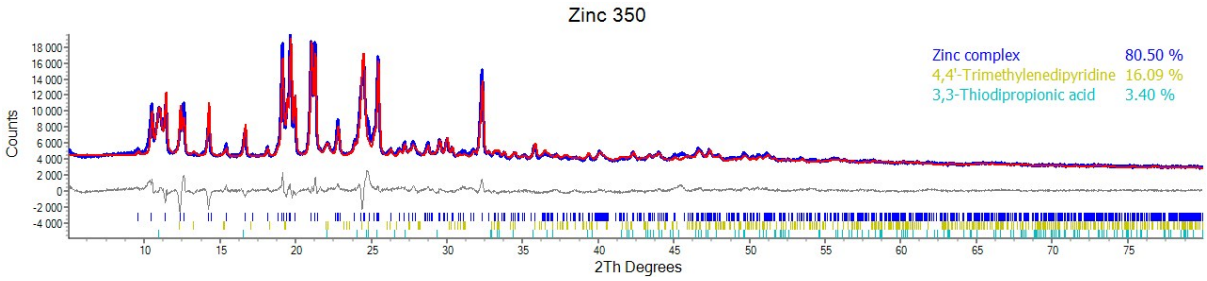

Fig. S3. (a) PXRD patterns of $[Zn(TDPA)_2(TMPy)_2]_n$ at room temperature; 150°C and 350°C under N_2 atmosphere (2Θ=30-70), (b) Phase quantification of $[Zn(TDPA)_2(TMPy)_2]_n$ at room temperature; 150°C and 350°C.

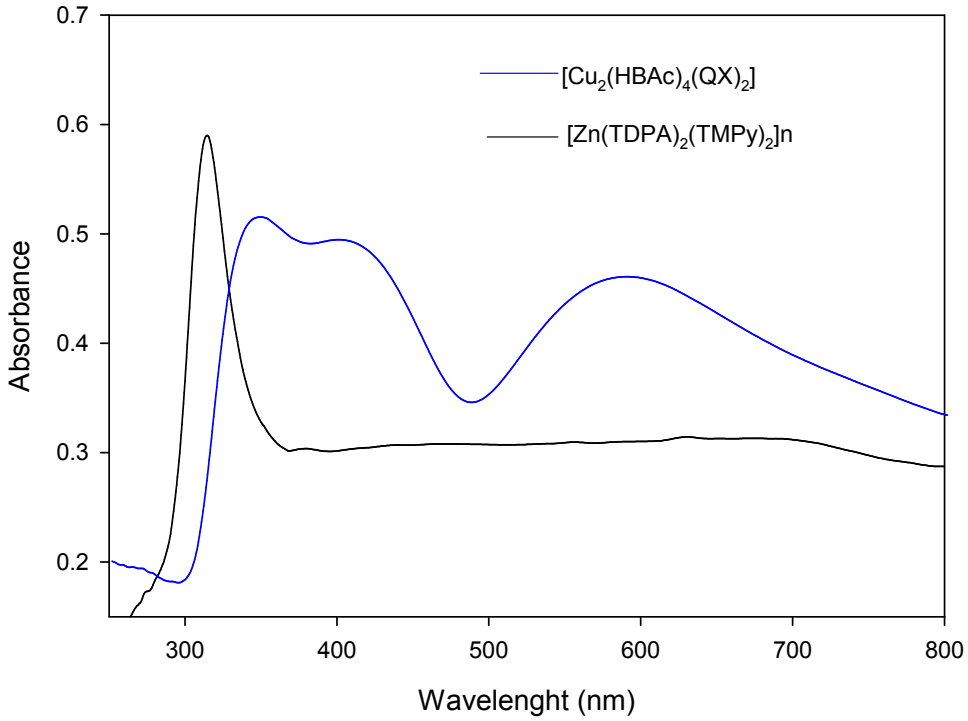

Fig. S4. Solid state UV-Vis spectra of $[Cu_2(BAc)_4(QX)_2]$ and $[Zn(TDPA)_2(TMPy)_2]_n$

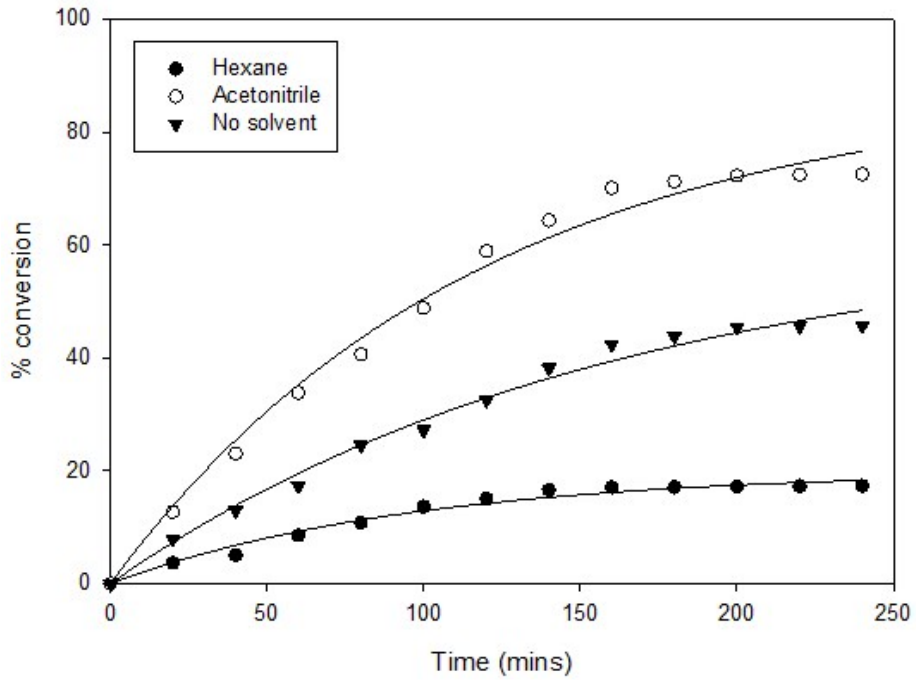

Fig. S5. Effect of solvent (acetonitrile and hexane) in the oxidation of DBT. $[H_2O_2]$ = 50 mmol; $[Cu_2(BAc)_4(QX)_2]$= 0.05 mmol; [DBT] = 10 mmol; temp.: 70°C.

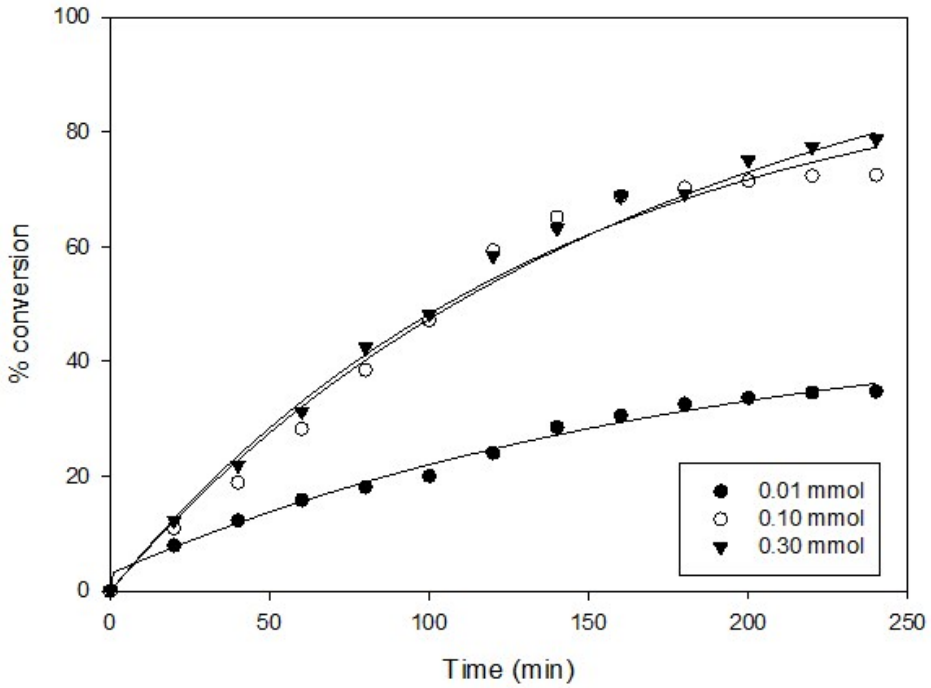

Fig. S6. Effect of $[Cu_2(BAc)_4(QX)_2]$ in the oxidation of DBT. $[H_2O_2]$ = 50 mmol; [DBT] = 10 mmol; temp.: 70°C; Acetonitrile= 10 mL

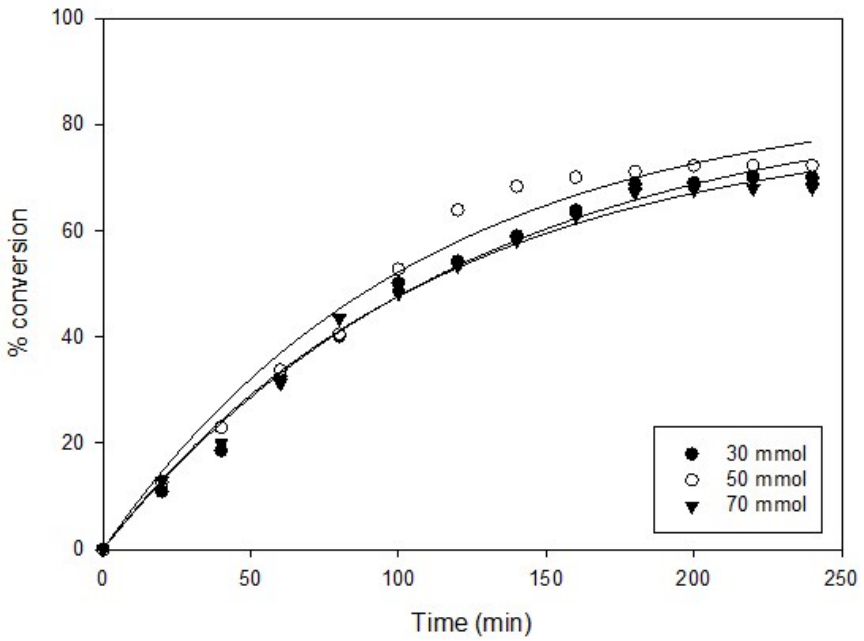

Fig. S7. Effect of oxidant (H_2O_2) in the oxidation of DBT. [$Cu_2(BAc)_4(QX)_2$]= 0.05 mmol; [DBT] = 10 mmol; temp.: 70°C; Acetonitrile = 10 mL

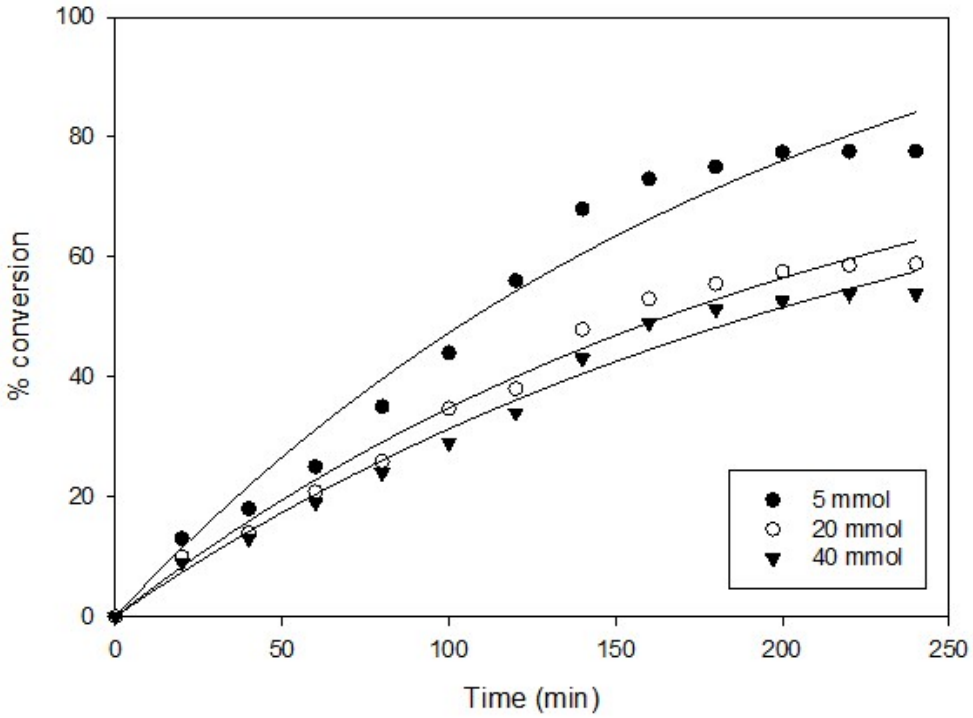

Fig. S8. Effect of DBT in the oxidation reaction. [H_2O_2] = 50 mmol; [$Cu_2(BAc)_4(QX)_2$]= 0.05 mmol; temp.: 70°C; Acetonitrile = 10 mL

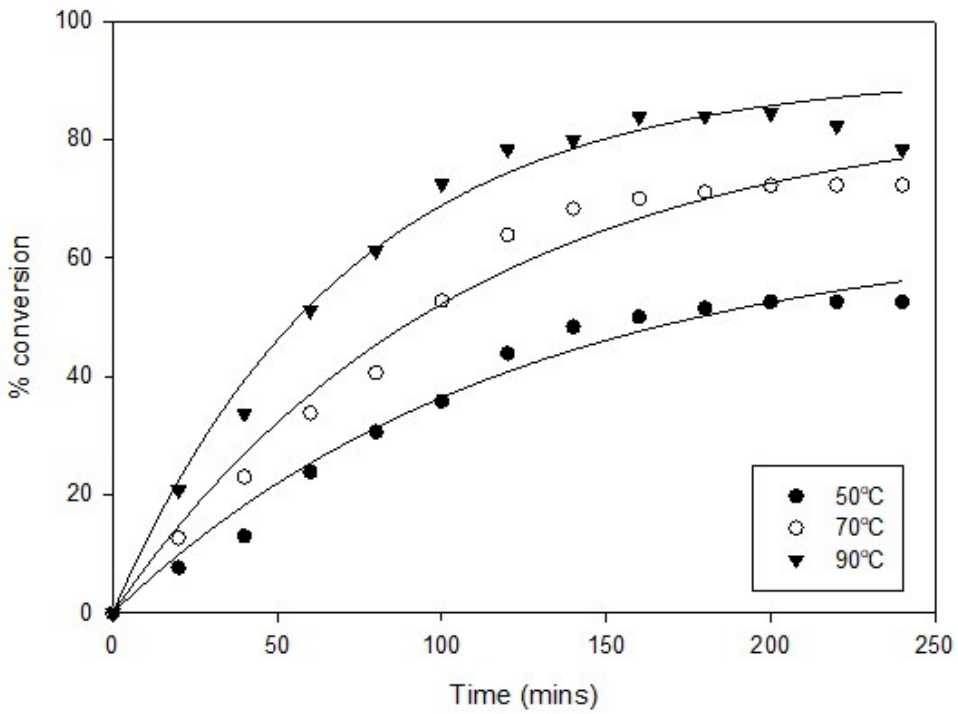

Fig. S9. Effect of temperature on the oxidation of DBT. $[H_2O_2]$ = 50 mmol; $[Cu_2(BAc)_4(QX)_2]$= 0.05 mmol; [DBT] = 10 mmol; Acetonitrile = 10 mL.

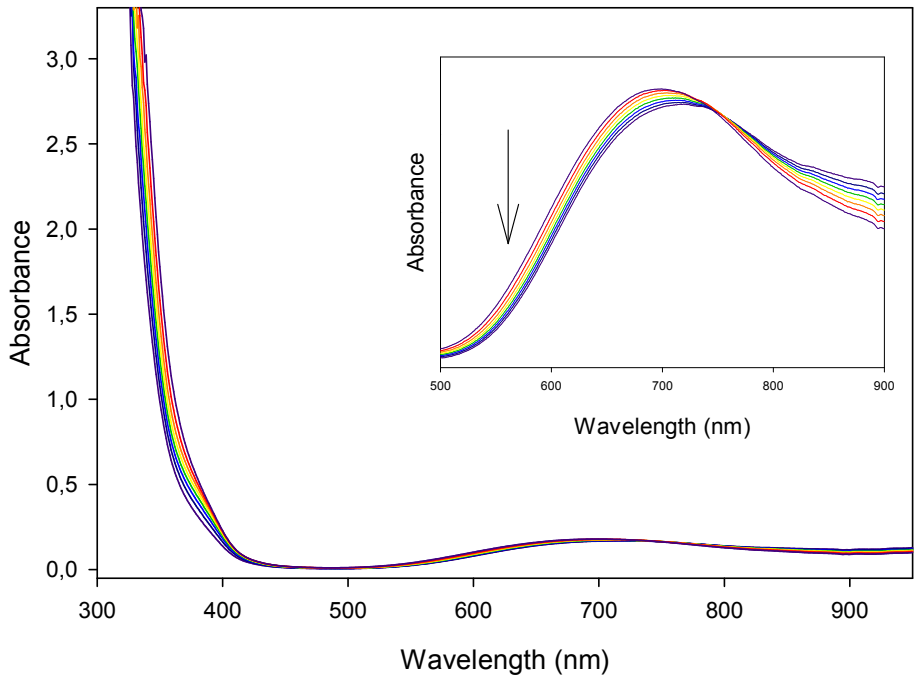

Fig. S10. UV-Vis studies showing the reaction between $[Cu_2(BAc)_4(QX)_2]$ and H_2O_2, $[Cu_2(BAc)_4(QX)_2]$.–H_2O_2 adduct]. Inset: Absorption spectra showing the decrease in d–d band region as reaction progresses.

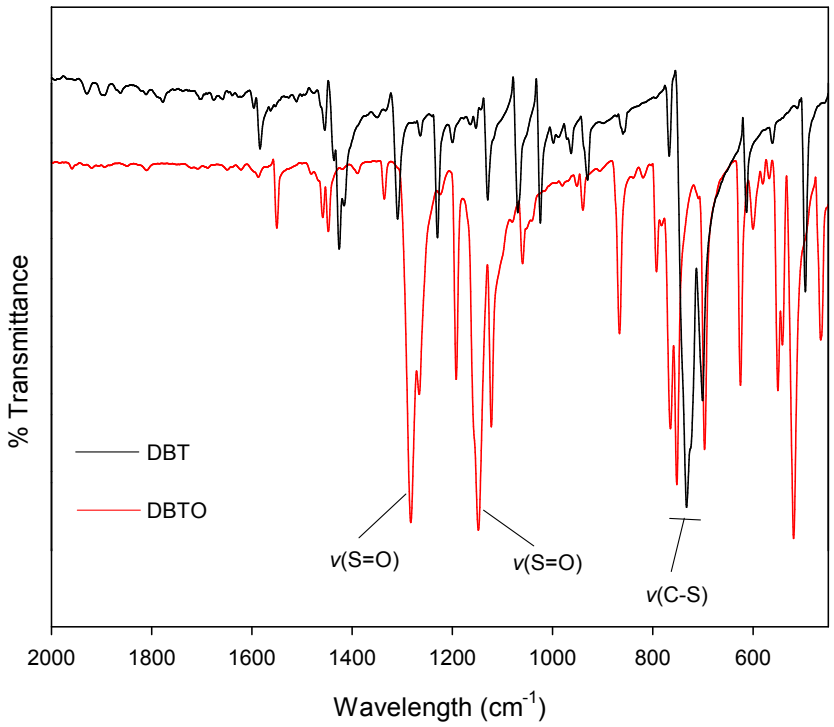

Fig. S11 FT-IR of Dibenzothiophene (DBT) and dibenzothiophene sulfoxide (DBTO).

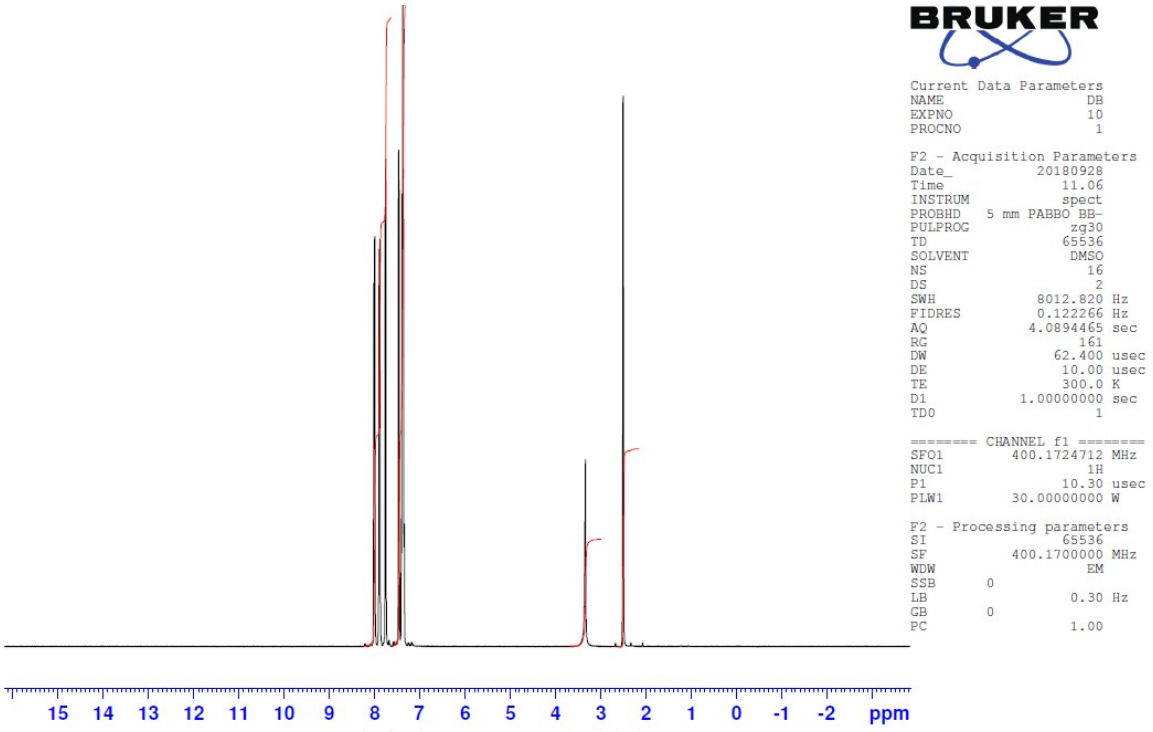

Fig. S12 ^{1}H NMR spectra of dibenzothiophene (DBT).

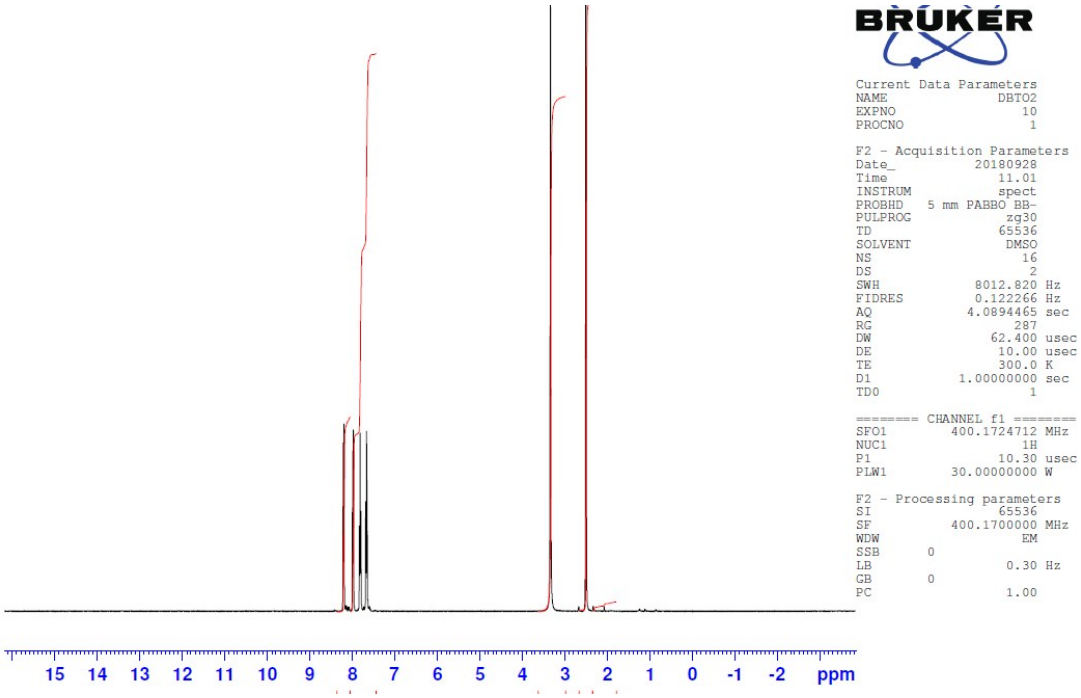

Fig. S13 ^{1}H NMR spectra of dibenzothiophene sulfoxide (DBTO).

Table S2 The calculated dipole moment (μ), mean polarizability (α_0), mean first-order molecular hyperpolarizability (β_0),HOMO–LUMO (eV), electronegativity (eV), hardness (eV), and softness (eV^{-1}) values of $[Zn(TDPA)_2(TMPy)_2]_n$.

	$[Zn(TDPA)_2(TMPy)_2]n$
First-order molecular hyperpolarizability	
β_{xxx}	751.16
β_{xyy}	2407.03
β_{xzz}	-198.72
β_{yyy}	9020.34
β_{xxy}	500.76
β_{yzz}	479.65
β_{zzz}	-223.76
β_{xxz}	-589.29
β_{yyz}	-1888.09
β_o ($\times 10^{-30}$ esu)	10773.57
Dipole moment	

μ_x	2.05
μ_y	55.20
μ_z	-27.80
M	61.84
Polarizability	
α_{xx}	-365.90
α_{xy}	235.65
α_{yy}	212.91
α_{xz}	76.97
α_{yz}	-136.27
α_{zz}	-380.85
A	-177.94
I	4.44
A	3.23
X	3.84
H	0.60
Σ	1.65

Table S3 Partial charge difference of some atoms in $[Zn(TDPA)_2(TMPy)_2]n$, DBT and DBTO before and after interaction

$[Zn(TDPA)_2(TMPy)_2]$ n		**$[Zn(TDPA)_2(TMPy)_2]n$ - DBT**		**$[Zn(TDPA)_2(TMPy)_2]$ n -DBTO**		**DBTO**		**DBT**	
O	-0.50	O	-0.49	O	-0.49	-	-	-	-
O	-0.50	O	-0.50	O	-0.50	-	-	-	-
O	-0.60	O	-0.56	O	-0.56	-	-	-	-
O	-0.41	O	-0.43	O	-0.43	-	-	-	-
Zn	1.15	Zn	0.95	Zn	0.94	-	-	-	-
Zn	0.90	Zn	0.89	Zn	0.89	-	-	-	-
-	-	S	0.20	S	0.40	S	1.04	S	0.29
-	-	-	-	O	-0.61	O	-0.92	-	-

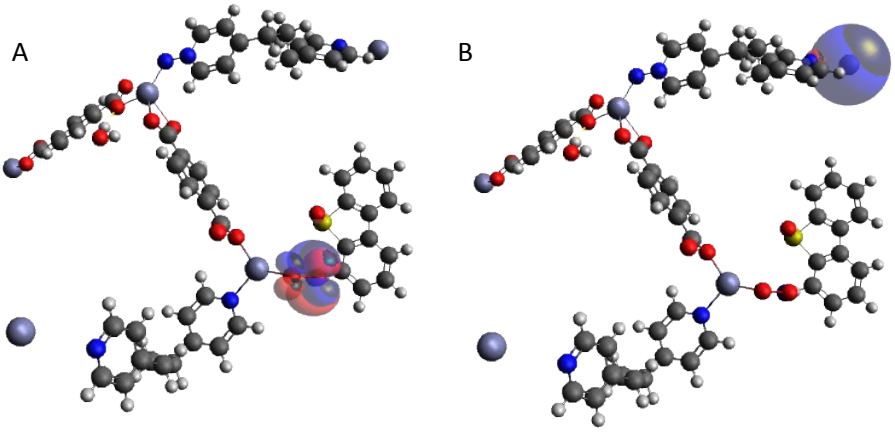

HOMO=-4.454 eV LUMO=-3.258 eV

Fig. S14. Optimized geometry of a unit of $[Zn(TDPA)_2(TMPy)_2]_n$ and DBTO adduct with respective (A) HOMO and (B) LUMO positions.

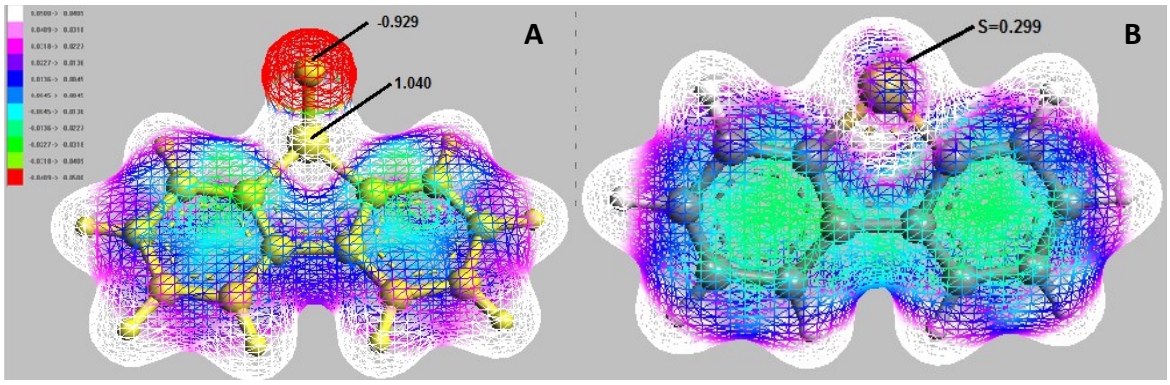

Fig. S15. Electrostatic potential mapping of sulfur and oxygen atoms on DBT and DBTO.

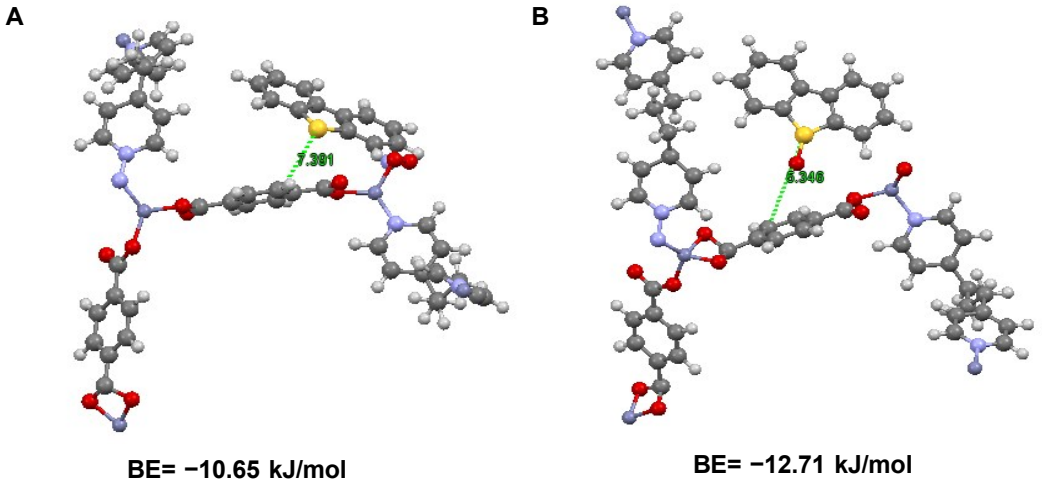

Fig. S16. Adsorption interaction conformations and binding energies (BEs) of (a) DBT and (b) DBTO with $[Zn(TDPA)_2(TMPy)_2]n$.

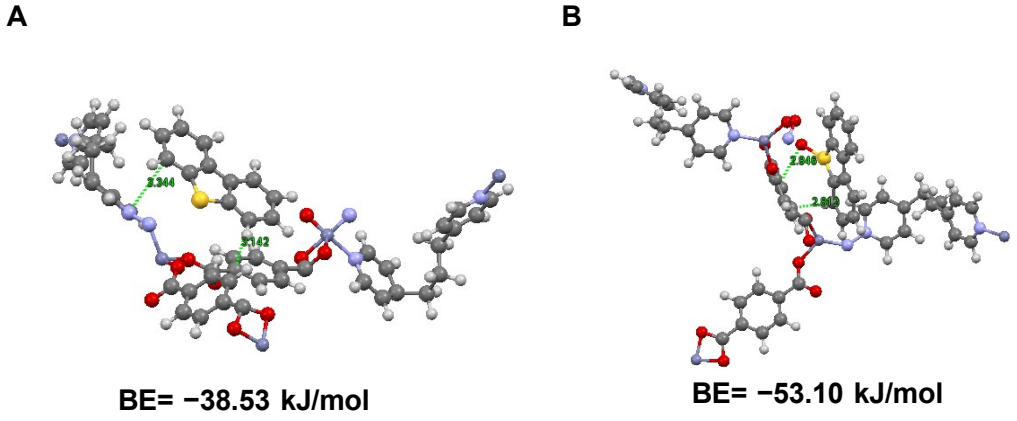

Fig. S17. Adsorption interaction conformations and binding energies (BEs) of (a) DBT and (b) DBTO with $[Zn(TDPA)_2(TMPy)_2]n$.

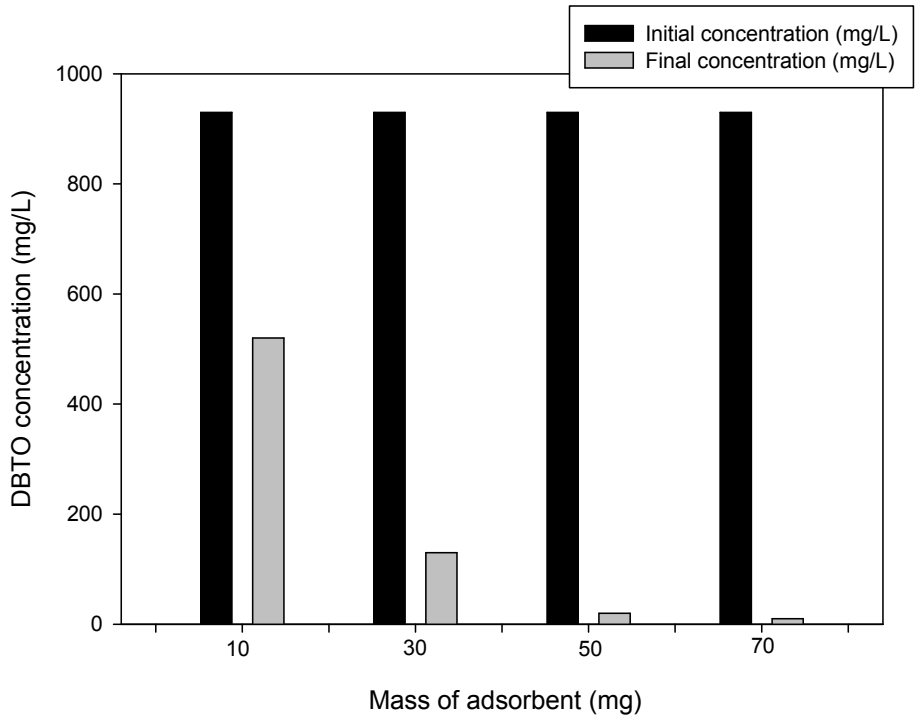

Fig. S18. (A) Amount of DBTO adsorbed by varying adsorbent mass ($[Zn(TDPA)_2(TMPy)_2]_n$) at constant time of 24 h at 25˚C.

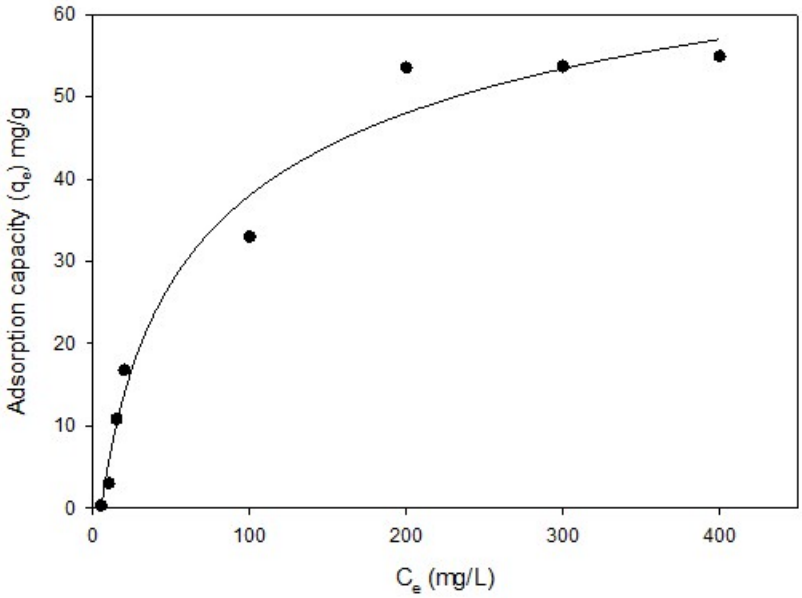

Fig. S19. Quantity of DBTO adsorbed by $[Zn(TDPA)_2(TMPy)_2]_n$ at different concentrations at 25˚C using 50 mg of adsorbent with a constant time of 24 h.

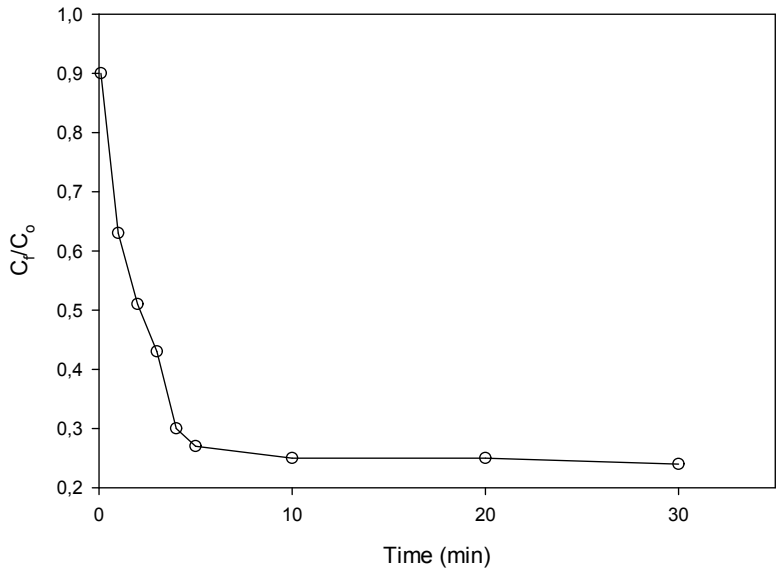

Fig. S20. Variation in DBTO concentrations by $[Zn(TDPA)_2(TMPy)_2]_n$ adsorption as a function of time at 25˚C, using 50 mg of adsorbent and 5 mL of 300 mg/L DBTO.

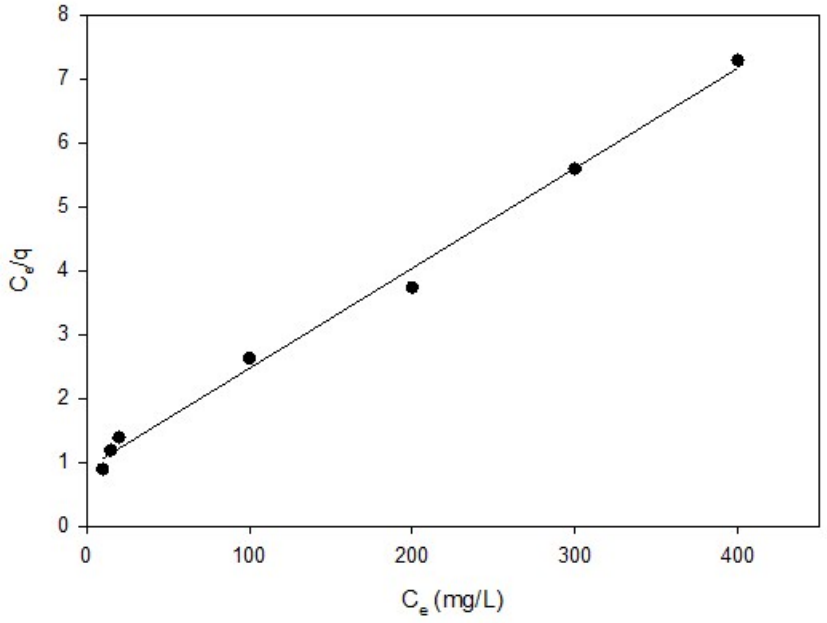

Fig. S21. Langmuir adsorption isotherms of DBTO over $[Zn(TDPA)_2(TMPy)_2]_n$.

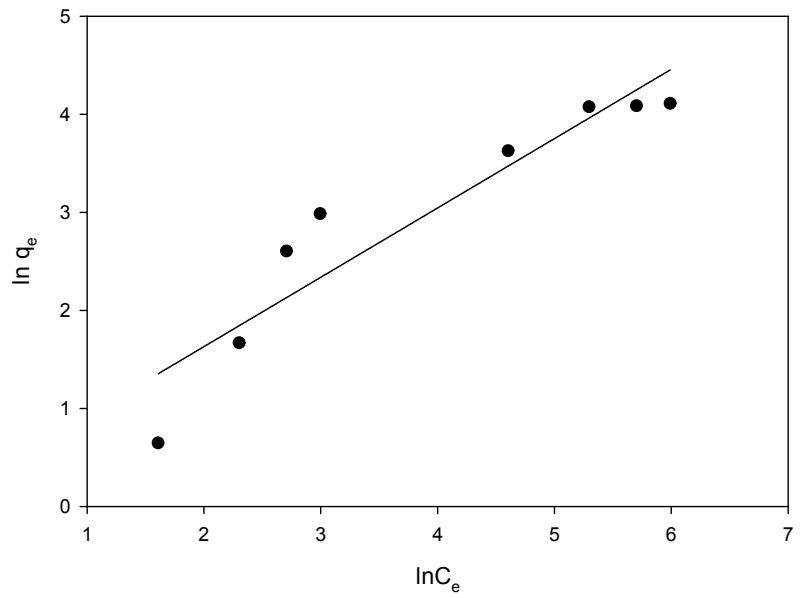

Fig. S22 Freudlich adsorption isotherms of DBTO over $[Zn(TDPA)_2(TMPy)_2]n$.

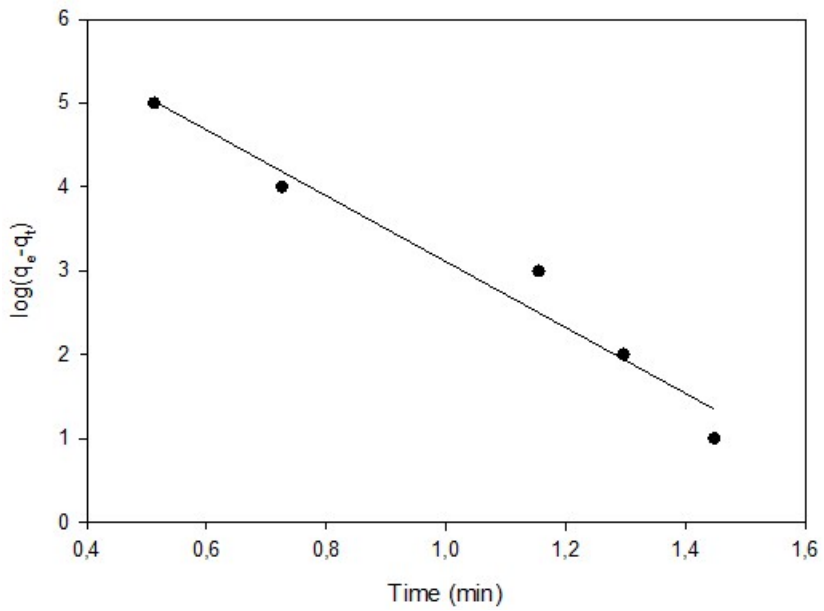

Fig. S23 Graph of log (q_e – q_t) vs. time

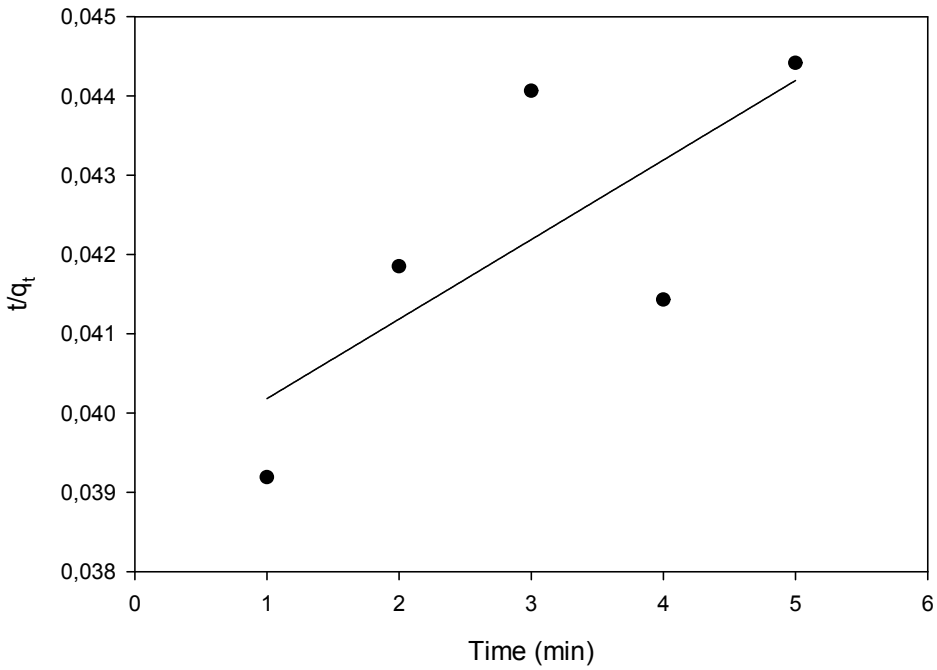

Fig. S24 Graph of t/ q_t vs. time

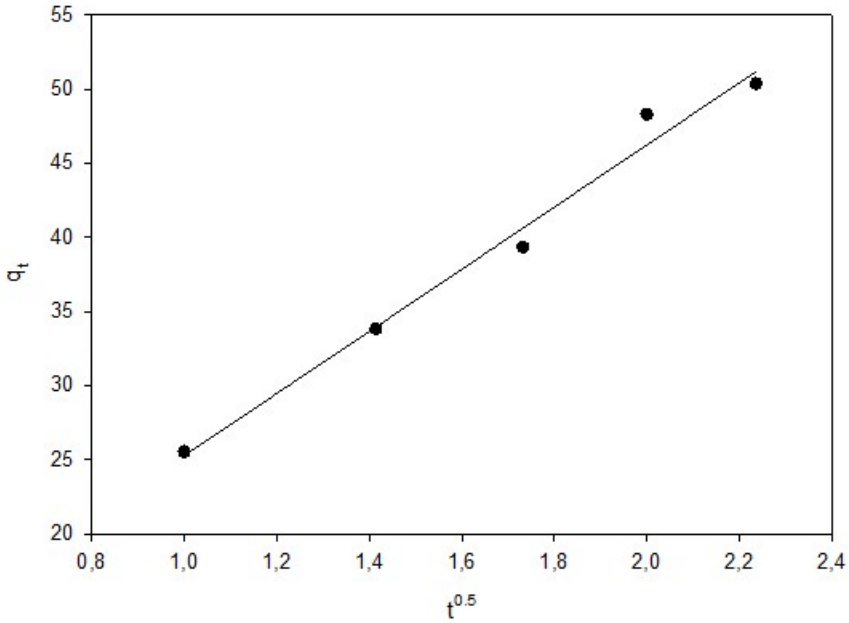

Fig. S25. Graph of q_t vs. time$^{0.5}$

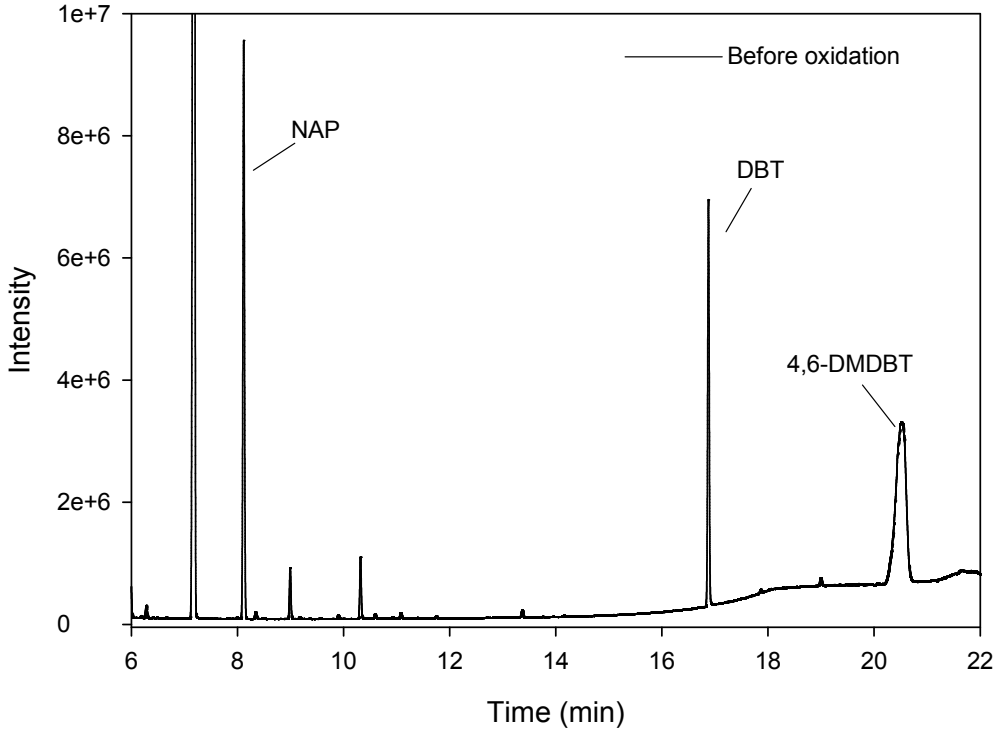

Fig. S26: GC-FID chromatograms of model fuel containing DBTO (930 mg/L), NAP (1000 mg/L), and 4,6-DMDBT (400 mg/L) in n-octane/acetonitrile mixture.

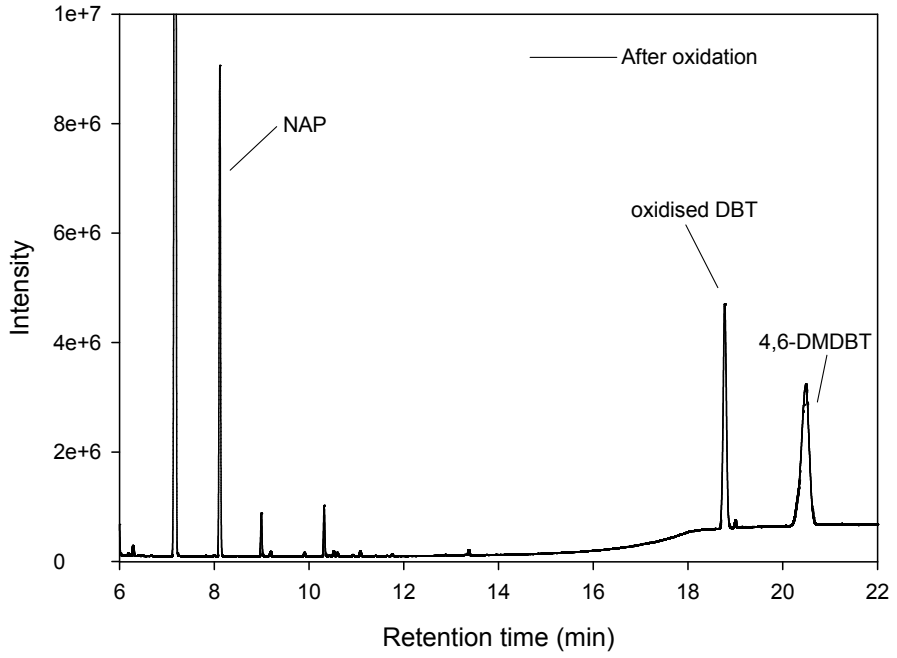

Fig. S27: GC-FID chromatograms of oxidized model fuel in n-octane/acetonitrile mixture (DBT (930 mg/L, 138 ppmS), 4,6-DMDBT (400 mg/L, 52.7 ppmS) and NAP (1000 mg/L)).

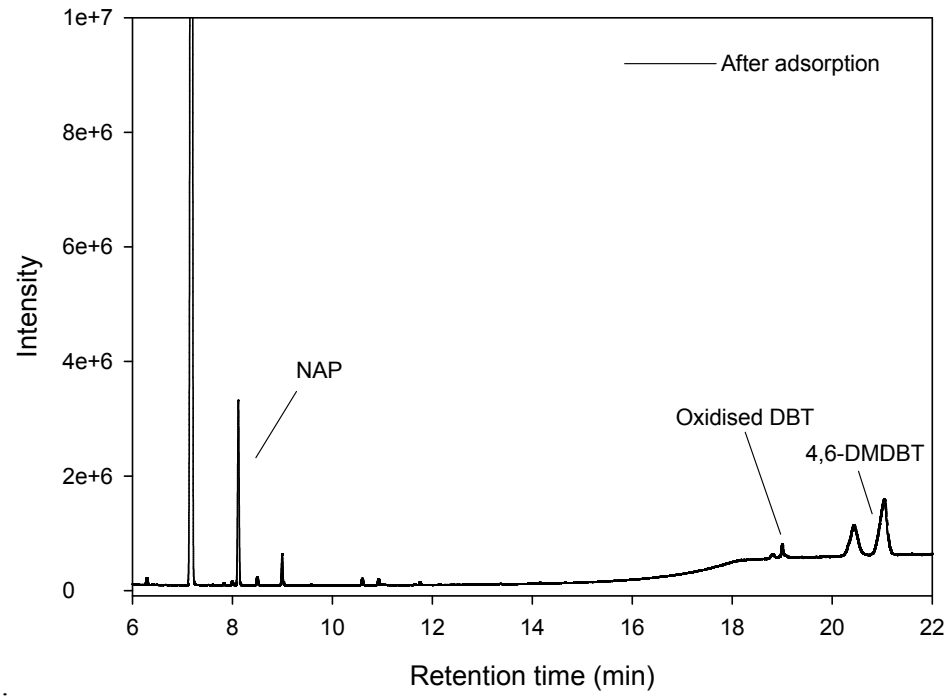

Fig. S28: GC-FID chromatograms of model fuel after adsorption (DBTO (101.37 mg/L, 15.1 ppmS), 4,6-DMDBT (188 mg/L, 24.8 ppmS) and NAP (640 mg/L)).

References

[1] S. Rajagopal, T.L. Grimm, D.J. Collins, R. Miranda, J. Catal. 137 (1992) 453−461.

[2] A.D. Becke, J. Chem. Phys. 98 (1993) 5648-5652.

[3] C. Lee, W. Yang, R.G. Parr, Phys. Rev. B 37 (1988) 785-789.

[4] M.J. Frisch, G.W. Trucks, H.B. Schlegel, G.E. Scuseria, M.A. Robb, J.R. Cheeseman, G. Scalmani, V. Barone, B. Mennucci, G.A. Petersson, H. Nakatsuji, M. Caricato, X. Li, H.P. Hratchian, A.F. Izmaylov, J. Bloino, G. Zheng, J.L. Sonnenberg, M. Hada, M. Ehara, K. Toyota, R. Fukuda, J. Hasegawa, M. Ishida, T. Nakajima, Y. Honda, O. Kitao, H. Nakai, T. Vreven, J.A. Montgomery, Jr., J.E. Peralta, F. Ogliaro, M. Bearpark, J.J. Heyd, E. Brothers, K.N. Kudin, V.N. Staroverov, R. Kobayashi, J. Normand, K. Raghavachari, A. Rendell, J.C. Burant, S.S. Iyengar, J. Tomasi, M. Cossi, N. Rega, J.M. Millam, M. Klene, J.E. Knox, J.B. Cross, V. Bakken, C. Adamo, J. Jaramillo, R. Gomperts, R.E. Stratmann, O. Yazyev, A.J. Austin, R. Cammi, C. Pomelli, J.W. Ochterski, R.L. Martin, K. Morokuma, V.G. Zakrzewski, G.A. Voth, P. Salvador, J.J. Dannenberg, S. Dapprich, A.D. Daniels, Ö. Farkas, J.B. Foresman, J.V. Ortiz, J. Cioslowski, and D.J. Fox, Gaussian 09, Revision D.01. Gaussian Inc., Wallingford CT, 2009.